GEOCHEMISTRY, MINERALOGY AND PETROLOGY • SOFIA
ГЕОХИМИЯ, МИНЕРАЛОГИЯ И ПЕТРОЛОГИЯ • СОФИЯ
2006, **44**, 91-102.

Characteristic of phenocryst assemblages in Sheinovets caldera rhyolite lava, Eastern Rhodopes, Bulgaria

Rositsa Ivanova

Abstract. Phenocrysts assemblages from the Sheinovets caldera rhyolite bodies were studied. Although all the samples are chemically undistinguishable, four phenocryst assemblages were detected: plagioclase+ biotite+sanidine+amphibole, plagioclase±biotite, sanidine+plagioclase+biotite+quartz and plagioclase+ biotite+clinopyroxene+sanidine. Differences in crystallization history of the rhyolites were proposed to explain observed variety in phenocrysts assemblages. The presence of amphibole phenocrysts indicates magma storage within amphibole stability field and rapid ascent preventing amphibole from breaking down. The existence of another magma holding reservoir at shallow levels or shallowing of the magma reservoir and ascending of its upper parts above the amphibole stability field is supposed to explain features of plagioclase±biotite containing rhyolites. The small amount of phenocrysts in these bodies is thought to suggest near liquidus temperature and non-eutectic crystallization of the erupting magma. The lack of quartz and sanidine phenocrysts can also be due to the longer nucleation-lag times in rhyolitic melts. Observed zones of sanidine (Or_{99-100}) in some plagioclase crystals, reflecting significant increase in potassium activity, are thought to result from contamination by high-potassium magma or assimilation of K-rich wall rock material. Quartz+sanidine-containing assemblage can be due to crystallization at low pressure resulting from slow magma ascent accompanied by significant cooling. Pyroxene-containing association was stable in deeper, probably both hotter and drier parts of the reservoir where significant contamination by less evolved magma might have occurred. Processes of magma mixing can also explain the observed internal dissolution surfaces associated with compositional amplitudes of over 20% An in pyroxene-accompanying plagioclase phenocrysts.

Key words: phenocryst assemblages, high-silica rhyolite, Paleogene volcanism, Eastern Rhodopes

Address: Geological Institute, Bulgarian Academy of Sciences, 1113 Sofia, Bulgaria;
E-mail: rossiv@geology.bas.bg

Росица Иванова. Характеристика на порфирните асоциации в риолитите от Шейновецката калдера, Източни Родопи, България

Резюме. Изследвани са порфирните асоциации в риолитите от Шейновецката калдера. Въпреки че всички образци са твърде сходни по състав, установени са четири асоциации от фенокристали: плагиоклаз+биотит+санидин+амфибол, плагиоклаз±биотит, санидин+плагиоклаз+биотит+кварц и плагиоклаз+биотит+клинопироксен+санидин. Вероятна причина за наблюдаваното разнообразие в порфирните асоциации са различия в кристализационната история на лавовите скали. Присъствието на амфибол е индикация за акумулация на магма в областта на стабилност на амфибола и бързо издигане, което позволява появата му в приповърхностни условия. Съществуване на по-плитко разположена камера или издигане на горните части на магмената камера над областта на стабилност на амфибола може да обясни липсата му в телата, съдържащи само плагиоклаз и биотит. Малкото количество на порфирите в тях вероятно се дължи на ликвидусна кристализация далеч от евтектиката. Липсата на кварц и санидин може да е следствие и на забавеното зародишообразуване във вискозните риолитови топилки. Зоните от санидин (Or_{99-100}), установени в някои плагиоклазови кристали, отразяват периоди на значително увеличение в активността на калия, причинено отсмесване с ултракалиева магма или асимилация на богат на калий материал от стените на магмената камера. Асоциации с участие на кварц и санидин възникват при кристализация при ниски налягания, в резултат на бавно издигане на магмата, придружено от значително охлаждане. Пироксен-съдържащата асоциация е била стабилна в по-дълбоките и сухи части на камерата, контаминирани значително от по-базични топилки. Процеси на магмено смесване обясняват и наблюдаваните в плагиоклазовите порфири от тази асоциация повърхнини на разтваряне и съществени вариации (над 20% An) в състава.

Introduction

Domes and dykes of high-silica rhyolites (72-79% SiO_2) are exposed within the area between Malko Gradishte, Mezek and Vulche Pole villages, approximately 10 km southwest of the town of Svilengrad (Ivanov, 1960; Yanev et al., 1983; Yanev, 1998; Ivanova, 2005). Built up mainly of pyroclastic flow deposits the area is thought to represent a fragment of a large Paleogene caldera, called Sheinovets (Yanev, 1995), lately uplifted as an element of the younger Ibredjeck horst. Strongly altered subvolcanic rhyolite dykes and sill-like bodies are emplaced within the coarse grained Priabonian sediments exposed in the caldera rim (Fig. 1). Regarding their K-Ar age (Ivanova et al., 2001) two groups of rhyolite bodies can be distinguished: Priabonian, including both domes and dykes exposed to the south and southeast of Malko Gradishte village, and Rupelian – all bodies and dykes from the southern parts of the area. More detailed information on geological setting of the Sheinovets caldera and petrology of volcanic products is reported in Ivanova (2005).

The studied rhyolite lava is scarcely porphyritic, pink or gray in colour. Normally observed phenocryst contents range from less than 5% to nearly 30-35%. Four phenocryst assemblages were detected:

plagioclase+biotite+sanidine+amphibole (found in phenocrysts-rich rhyolite blocks within the pyroclastic section),

plagioclase±biotite,

sanidine+plagioclase+biotite+quartz and

plagioclase+biotite+clinopyroxene+sanidine.

This paper focuses on the features of phenocrysts and their associations since they record variations in *T-P*-time paths of the rising separate magma batches. Phenocryst composition was obtained using JEOL 733 Superprobe at the Geological Institute (by Tz. Iliev) and Cameca SX 100 electron probe microanalyser at the Institute of Petrology, Vienna University.

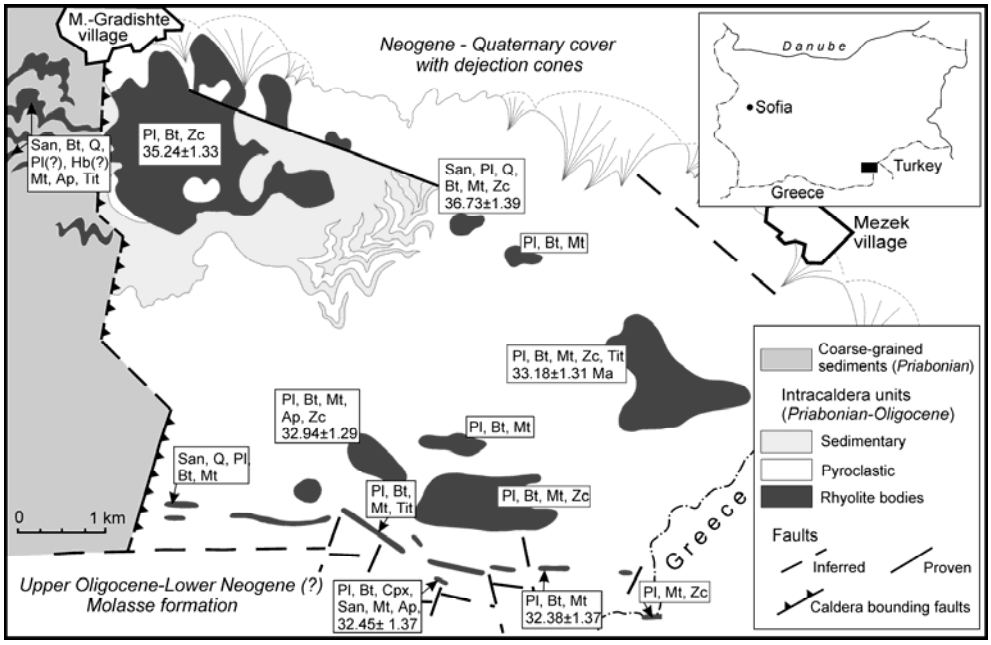

Fig. 1. Simplified geological map of the Sheinovets caldera (modified from Ivanova et al., 2000). Phenocrysts and accessories present in the rhyolite bodies are also shown (Pl-plagioclase, Bt-biotite, Kfs-sanidine, Hb-amphibole, Px-pyroxene, Q-quartz, Mt-magnetite, Zc-zircon, Ap-apatite, Tit-titanite). K-Ar age (in Ma) is after Ivanova et al., (2001)

Фиг. 1. Схематична карта на Шейновецката калдера (по Ivanova et al., 2000). Установените в отделните риолитови тела порфири и акцесорни минерали също са показани (Pl-плагиоклаз, Bt-биотит, Kfs-санидин, Hb-амфибол, CPx-клинопироксен, Q-кварц, Mt-магнетит, Zc-циркон, Ap-апатит, Tit-титанит). K-Ar възраст (в Ma) е по Ivanova et al., (2001)

Phenocryst characteristic

Plagioclase+biotite+sanidine+amphibole association

As it was mentioned above, this association is found in large rhyolite blocks that were ejected during explosive phases preceding dome activity and are, probably, parts of bodies solidified at some depth below the surface. This resulted both in phenocrysts abundance (30-35%) and larger sizes of the crystals.

The main phenocryst of plagioclase is occurring as large (up to 5 mm) euhedral to subhedral crystals, sometimes forming crystal clots together with biotite and amphibole. The most of plagioclase crystals show zonal textures having slightly resorbed cores (An_{55-53}) mantled by oscillatory-zoned peripheries (An_{46-25}). The composition of the outermost surface is An_{30-33} (Table 1, Fig. 2A). Large (up to 3-4 mm) coarse sieve textured crystals (An_{33}), showing no zonality neither compositional variation, are also present. Large (up to 6 mm) sanidine phenocrysts are very common. They are euhedral to subhedral, often twinned. Normally obtained orthoclase contents are Or_{71-72}. Values of Or_{99-100} were also detected in the

Table 1. *Representative feldspar compositions from the Sheinovets caldera rhyolites*
Таблица 1. *Представителни анализи на фелдшпати от риолитите от Шейновецката калдера*

	Plagioclase+biotite+sanidine+amphibole association								*Plagioclase±biotite association*				
Sample	158 (rhyolite lithoclasts)							75*	1 (rhyolite dome)				
	Pl in Hb	Pl-c	Pl-m_1	Pl-m_2	Pl-r	Pl-c	Pl-r	San	San	Pl-c	Pl-m	Pl-r_1	Pl-r_2
SiO_2	61.37	56.87	59.44	55.10	60.54	60.48	60.66	66.80	62.44	57.65	66.78	60.28	60.97
TiO_2	n.d	0.01	0.01	n.d.	0.01	n.d.	n.d.	0.03	0.04	0.02	0.01	0.04	n.d.
Al_2O_3	24.35	27.20	25.70	28.46	25.13	25.03	24.90	18.21	19.12	26.26	17.48	24.50	24.06
FeO	0.36	0.29	0.22	0.19	0.23	0.19	0.23	0.02	0.09	0.27	0.02	0.18	0.20
MnO	n.d.	0.02	0.02	n.d.	0.02	n.d	0.02	n.d.	n.d.	0.03	0.02	n.d.	0.01
MgO	0.02	0.01	0.02	n.d.	0.02	0.02	0.02	0.01	n.d.	0.02	n.d.	0.01	n.d.
CaO	5.92	9.35	7.40	10.81	6.60	6.63	6.59	0.01	0.16	8.33	0.05	6.30	5.63
Na_2O	7.36	5.74	6.58	5.03	6.90	6.97	6.93	0.02	2.36	6.48	0.04	7.43	7.64
K_2O	0.87	0.42	0.63	0.30	0.78	0.76	0.78	15.93	11.68	0.49	15.27	0.69	0.85
Total	100.25	99.91	100.02	99.89	100.23	100.08	100.13	101.03	95.89	99.55	99.67	99.43	99.36
An	29.2	46.2	36.9	53.3	33.0	32.9	32.9	0.1	0.9	40.4	0.3	30.6	27.5
Ab	65.7	51.3	59.4	44.9	62.4	62.6	62.5	0.2	23.3	56.8	0.4	65.4	67.6
Or	5.1	2.4	3.7	1.7	4.6	4.5	4.6	99.8	75.8	2.8	99.3	4.0	4.9

	Plagioclase±biotite association												
Sample	169 (rhyolite dome)			317 (perlite)						365 (rhyolite)			
	Pl-c	Pl-m	Pl-r	Pl-c	Pl-r	Pl-c_1	Pl-c_2	Pl-m	Pl-r	Pl-c	Pl-c	Pl-m_1	Pl-m_2
SiO_2	57.80	59.27	69.93	61.19	62.63	52.56	48.87	59.13	62.55	61.19	57.98	59.90	58.58
TiO_2	0.02	0.02	0.03	n.d.	0.03	0.01	0.02	0.01	0.01	n.d.	n.d.	0.04	0.02
Al_2O_3	22.29	20.97	15.29	24.68	23.84	30.18	32.95	26.39	23.71	24.68	26.00	25.10	25.96
FeO	0.22	0.21	0.15	0.19	0.19	0.26	0.26	0.20	0.18	0.19	0.21	0.23	0.24
MnO	n.d.	0.01	0.06	n.d.	0.01	0.03	0.01	n.d.	n.d.	n.d.	0.01	0.01	n.d.
MgO	0.01	0.01	n.d.	n.d.	n.d.	0.03	0.01	0.01	0.02	n.d.	0.02	0.02	n.d.
CaO	7.75	6.68	3.79	6.06	5.25	12.86	15.92	8.12	5.10	6.06	7.96	6.53	7.62
Na_2O	6.40	7.05	5.62	7.34	7.74	3.94	2.37	6.56	7.16	7.34	6.45	6.98	6.65
K_2O	0.44	0.51	0.60	0.68	0.88	0.18	0.08	0.47	1.40	0.68	0.49	0.71	0.57
Total	94.93	94.73	95.47	100.14	100.57	100.05	100.49	100.89	100.13	100.14	99.12	99.52	99.64
An	39.0	33.3	25.8	30.1	25.9	63.6	78.4	39.5	25.9	30.1	39.4	32.6	37.5
Ab	58.3	63.6	69.3	65.9	69.0	35.3	21.1	57.8	65.7	65.9	57.7	63.1	59.2
Or	2.6	3.0	4.9	4.0	5.2	1.0	0.5	2.7	8.4	4.0	2.9	4.2	3.3

	Plagioclase±biotite association						*Sanidine+plagioclase+biotite+quartz*						
Sample	365 (rhyolite)			63 (perlite)			89 (rhyolite dome)						
	Pl-r	Pl-c	Pl-r	Pl-c	Pl-m	Pl-r	Pl-c	Pl-m_1	Pl-m_2	Pl-r	Pl in San	San-c	San-r
SiO_2	59.68	61.26	60.49	55.59	60.46	60.29	63.54	63.44	64.05	63.37	63.68	64.69	65.03
TiO_2	n.d.	n.d.	n.d.	0.02	0.01	0.02	n.d.	0.01	n.d.	n.d.	n.d.	0.01	0.03
Al_2O_3	25.15	24.20	24.43	27.58	24.61	24.86	22.55	22.59	22.52	22.94	22.64	18.86	18.92
FeO	0.21	0.19	0.23	0.29	0.22	0.22	0.11	0.12	0.11	0.15	0.12	0.09	0.09
MnO	0.02	0.02	n.d.	n.d.	n.d.	0.03	0.01	n.d.	n.d.	0.02	0.01	n.d.	n.d.
MgO	0.02	n.d.	0.01	n.d.	n.d.	0.01	n.d.	n.d.	n.d.	n.d.	n.d.	n.d.	0.03
CaO	6.51	5.73	6.10	9.71	6.12	6.30	3.51	3.56	3.28	3.78	3.66	0.14	0.13
Na_2O	7.08	7.46	7.31	5.48	7.35	7.18	8.64	8.55	8.63	8.38	8.63	3.21	3.13
K_2O	0.66	0.85	0.77	0.39	0.74	0.68	1.05	0.96	1.00	0.94	1.01	11.55	11.74
Total	99.34	99.72	99.34	99.07	99.51	99.59	99.41	99.23	99.59	99.58	99.75	98.55	99.10
An	32.4	28.3	30.1	48.3	30.1	31.4	17.2	17.6	16.3	18.8	17.9	0.7	0.7
Ab	63.7	66.7	65.3	49.4	65.5	64.6	76.6	76.7	77.7	75.6	76.3	29.5	28.7
Or	3.9	5.0	4.5	2.3	4.3	4.0	6.2	5.7	5.9	5.6	5.8	69.8	70.7

* – strongly altered rhyolite dyke from the caldera rim; c – core, m – medial zones, r – rim; * – силно променена риолитова дайка от рамката на калдерата; c – ядро, m – междинни зони, r – периферия

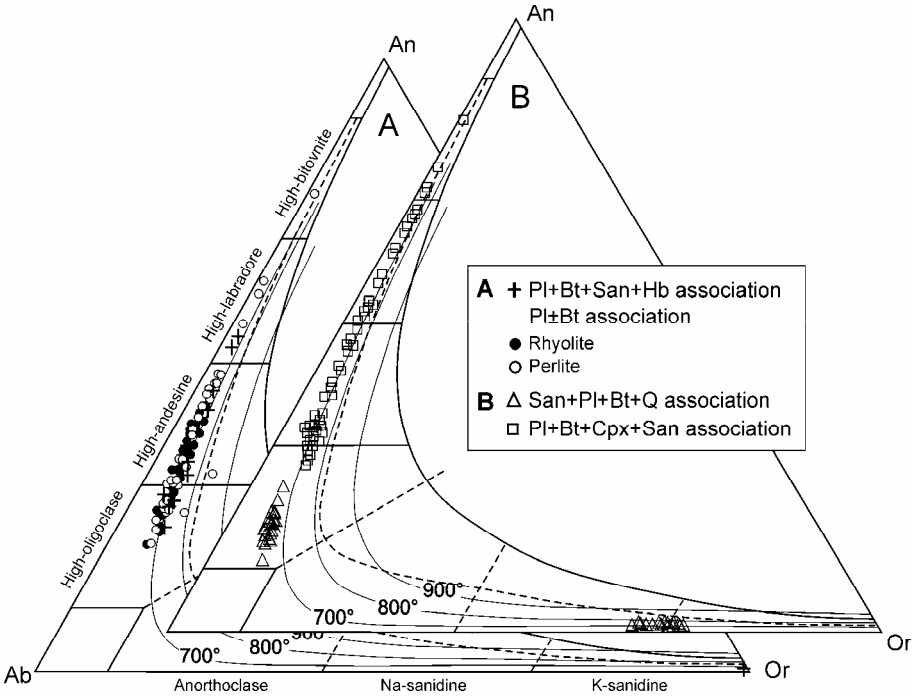

Fig. 2. Range in composition of feldspars from Sheinovets caldera rhyolites plotted in An-Ab-Or diagram. The isotherms (1 kbar) shown are after Elkins & Grove (1990) and Wen & Nekvasil (1994). Pl - plagioclase; Bt - biotite; San - sanidine; Hb - amphibole; Q - quartz; Cpx - clinopyroxene

Фиг. 2. Вариации в състава на фелдшпатите в риолитите от Шейновецката калдера. Показаните изотерми (1 kbar) са по Elkins & Grove (1990) и Wen & Nekvasil (1994). Pl – плагиоклаз, Bt – биотит, San – санидин, Hb – амфибол, Q – кварц, Cpx – клинопироксен

peripheries of feldspars having strongly resorbed cores and forming a crystal clot. Fragments of plagioclase and sanidine are very abundant as both large subhedral fragments of broken crystals and tiny angular splinters, derived from strongly cracked crystals, can be seen. Biotite (Table 2) forms small (≤1 mm) flakes dispersed in the groundmass or included in the clots. Amphibole (magnesiohornblende, according to the classification of Leake et al., 1997, Table 3) occurs as large (2-3 mm) euhedral to subhedral crystals, sometimes grown over biotite, or smaller anhedral grains within the clots. The accessory minerals detected are magnetite, titanite and zircon. The groundmass is felsitic enriched in feldspar and biotite microliths.

Amphibole must also have been present in the altered subvolcanic bodies from the Sheinoevets caldera rim as indicated by the well-preserved pseudomorphic opacite rims. Development of reaction rims over biotite and amphibole grains and complete decomposition of amphibole crystals had occurred prior to final magma emplacement. Plagioclase was replaced by calcite, albite and clay minerals

Table 2. *Selected analyses of biotite from the Sheinovets caldera rhyolites. Structural formulae based on 22 oxygen.*
Таблица 2. *Избрани анализи на биотити в риолитовите скали от Шейновецката калдера. Кристалохимичните формули са изчислени при O=22*

																San+Pl+Bt+Q			
Sample	158		75		1		169		317		365		63		89	198	254	
SiO_2	36.89	36.98	35.35	36.02	36.38	35.91	36.93	36.18	37.47	36.88	36.69	36.17	36.04	36.85	36.15	36.33	35.06	36.19
TiO_2	4.68	4.50	4.40	4.02	4.02	4.14	4.09	4.27	4.49	4.55	4.37	4.32	4.38	4.21	4.03	4.13	5.04	4.96
Al_2O_3	13.87	13.28	13.99	13.81	14.06	14.24	12.42	12.09	13.71	13.88	13.83	14.34	14.61	13.82	14.10	14.00	14.28	13.46
FeO	16.23	16.29	18.83	18.47	16.76	17.18	16.17	16.94	16.05	16.37	15.38	15.95	15.65	15.01	17.58	17.77	16.79	15.64
MnO	0.43	0.49	0.52	0.53	0.65	0.66	0.62	0.71	0.60	0.64	0.61	0.57	0.54	0.51	1.22	1.25	0.47	0.44
MgO	13.76	14.11	11.61	12.25	13.92	13.53	14.25	13.33	13.90	13.52	14.77	13.92	13.86	13.85	12.27	12.39	12.98	13.88
CaO	0.01	0.04	0.02	n.d.	0.01	n.d.	0.01	0.02	n.d.	0.01	n.d.	0.02	0.03	0.15	0.01	n.d.	0.01	0.03
Na_2O	0.42	0.42	0.29	0.32	0.39	0.44	0.45	0.61	0.44	0.41	0.41	0.41	0.43	0.33	0.34	0.36	0.49	0.39
K_2O	8.76	8.25	8.65	9.00	8.48	8.93	8.78	8.72	8.60	8.98	8.80	8.58	8.60	7.78	9.02	9.23	8.71	7.68
Total	95.05	94.36	93.67	94.43	94.67	95.02	93.72	92.87	95.27	95.23	94.85	94.28	94.14	92.50	94.72	95.47	93.86	92.66
K	1.69	1.60	1.72	1.77	1.64	1.74	1.72	1.74	1.65	1.73	1.69	1.67	1.67	1.52	1.77	1.80	1.71	1.51
Na	0.12	0.12	0.09	0.10	0.11	0.13	0.13	0.18	0.13	0.12	0.12	0.12	0.13	0.10	0.10	0.11	0.15	0.12
Ca	-	0.01	-	-	-	-	-	-	-	-	-	-	-	0.02	-	-	-	-
	1.81	1.73	1.81	1.87	1.76	1.87	1.85	1.92	1.78	1.85	1.81	1.79	1.80	1.64	1.87	1.90	1.86	1.63
Mg	3.10	3.19	2.69	2.81	3.15	3.07	3.26	3.10	3.11	3.04	3.32	3.16	3.14	3.16	2.81	2.82	2.98	3.18
Mn	0.06	0.06	0.07	0.07	0.08	0.09	0.08	0.09	0.08	0.08	0.08	0.07	0.07	0.07	0.16	0.16	0.06	0.06
Fe^{2+}	2.05	2.07	2.45	2.38	2.13	2.19	2.08	2.21	2.02	2.07	1.94	2.03	1.99	1.93	2.26	2.27	2.16	2.01
Al	0.03	-	0.07	0.06	0.05	0.03	-	-	0.05	0.04	-	0.07	0.10	0.15	0.10	0.06	-	-
Ti	0.53	0.51	0.51	0.47	0.46	0.47	0.47	0.50	0.51	0.52	0.50	0.49	0.50	0.49	0.47	0.47	0.58	0.57
	5.76	5.84	5.80	5.79	5.87	5.85	5.89	5.91	5.76	5.75	5.84	5.82	5.81	5.79	5.78	5.78	5.79	5.83
Si	5.57	5.61	5.50	5.55	5.53	5.47	5.67	5.65	5.63	5.57	5.54	5.50	5.48	5.65	5.55	5.54	5.40	5.56
^{IV}Al	2.43	2.39	2.50	2.45	2.47	2.53	2.33	2.35	2.37	2.43	2.46	2.50	2.52	2.35	2.46	2.46	2.60	2.44
	8.00	8.00	8.00	8.00	8.00	8.00	8.00	8.00	8.00	8.00	8.00	8.00	8.00	8.00	8.00	8.00	8.00	8.00
Mg/Mg+F	60.20	60.70	52.40	54.20	59.70	58.40	61.10	58.40	60.70	59.50	63.10	60.90	61.20	62.20	55.40	55.40	58.00	61.30
Mg/Fe	1.5	1.54	1.10	1.18	1.48	1.40	1.57	1.40	1.54	1.47	1.71	1.56	1.58	1.64	1.24	1.24	1.38	1.58

Table 3. *Composition of amphibole and pyroxene identified in the Sheinovets caldera rhyolites*
Таблица 3. *Състав на амфибол и пироксен, установени в риолитите от Шейновецката калдера*

	Hb (sample 158)				Cpx (sample 254)		
SiO_2	48.06	46.08	46.86	SiO_2	52.4	51.8	52.05
TiO_2	0.99	1.41	1.47	TiO_2	0.14	0.23	0.17
Al_2O_3	6.26	8.69	7.55	Al_2O_3	0.93	1.45	1.14
				Cr_2O_3	0.01	n.d	0.01
FeO	13.50	14.35	14.00	FeO	8.38	9.58	9.15
MnO	1.08	0.79	0.86	MnO	1.24	1.09	1.15
MgO	14.10	12.75	13.57	MgO	13.9	12.6	13.28
CaO	11.36	11.38	11.30	CaO	22.5	22.9	22.74
Na_2O	1.23	1.52	1.41	Na_2O	0.42	0.49	0.46
K^2O	0.53	0.93	0.74	K_2O	n.d.	n.d.	0.01
Total	97.10	97.90	97.76	Total	100.	100.	100.16
Si	6.99	6.73	6.81	Si^{4+}	1.95	1.94	1.94
^{IV}Al	1.01	1.27	1.20	^{IV}Al	0.04	0.06	0.05
^{VI}Al	0.06	0.22	0.10	Fe^{3+}	0.01	-	0.01
Ti	0.11	0.16	0.16	Al^{VI}	-	-	-
Fe^{3+}	0.75	0.58	0.73	Fe^{3+}	0.07	0.08	0.08
Mg	3.06	2.77	2.94	Ti^{4+}	-	0.01	0.01
Fe^{2+}	0.89	1.17	0.98	Mg^{2+}	0.78	0.70	0.74
Mn	0.13	0.10	0.11	Fe^{2+} (M1)	0.15	0.21	0.18
Ca	1.77	1.78	1.76	Fe^{2+} (M2)	0.03	0.01	0.02
Na (M4)	0.23	0.22	0.24	Mn^{2+}	0.04	0.03	0.04
Na (A)	0.35	0.21	0.40	Ca^{2+}	0.90	0.92	0.91
K	0.10	0.17	0.14	Na^{+}	0.03	0.04	0.03
Mg/Fe	0.77	0.70	0.75	mg	0.81	0.77	0.79

during later hydrothermal processes. The only preserved components of the original phenocryst association are sanidine, rounded quartz and some biotite showing lower $Mg/Mg+Fe_{tot}$ ratio.

Plagioclase±biotite association

This is the most common association observed in most of the Sheinovets caldera rhyolite bodies, both domes and dykes. Phenocryst contents are significantly lower, about 10% or even less than 5%. The plagioclase is always prevailing over biotite and usually occurs as cracked euhedral to subhedral crystals, less than 1 mm across. They show normal or reverse zoning with variation in An contents from An_{37} to An_{21} (Table 1, Figs. 2A and 3A). Larger plagioclase crystals (more than 1 mm in length) are also present in some of the samples and remnants of more basic plagioclase can be arrested in their central parts (Figs. 2A and 3B). Observed cores display various degree of resorption in different samples and range in composition between An_{39} and An_{78}. Zones, composed by almost pure potassium feldspar ($Or_{99.4}$) were detected in some of the plagioclase phenocrysts in one body. They can envelope the resorbed cores (An_{42}-An_{40}), or to build the central parts of the smaller phenocrysts (Fig. 3C). The same sample contains sanidine microliths (Or_{62-58}). Relatively large (>1mm) euhedral to subhedral coarse sieve-textured plagioclase phenocrysts displaying no zonal textures and only a weak

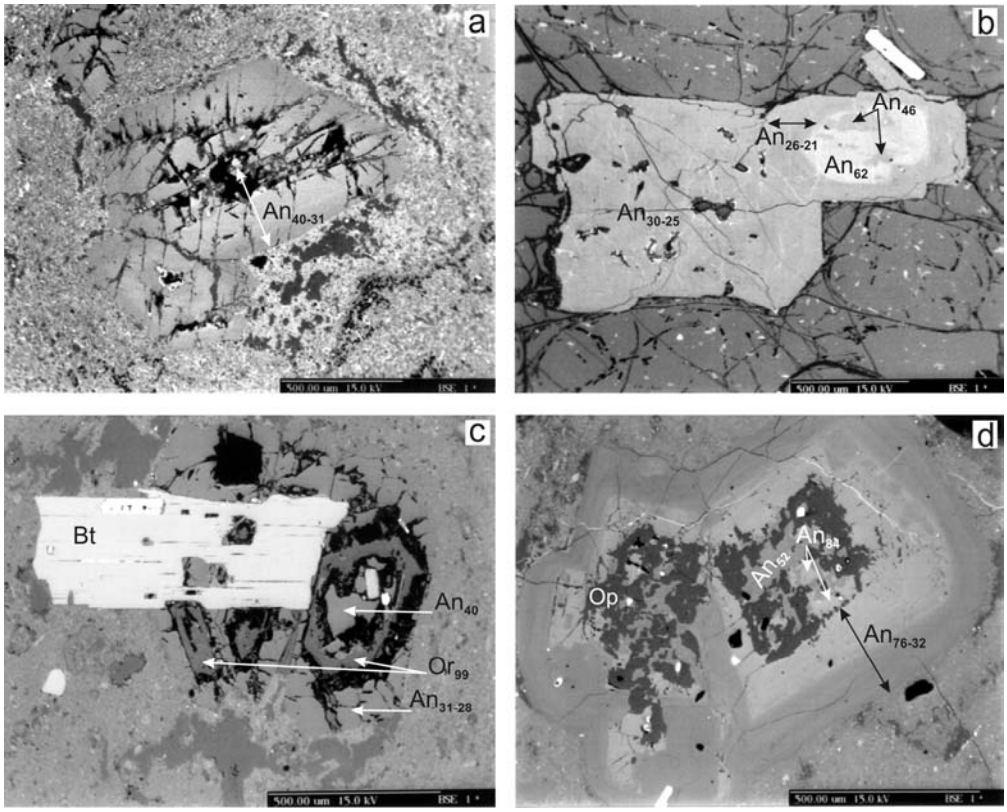

Fig. 3. Back-scattered electron images of different types of plagioclase phenocrysts from Sheinovets caldera rhyolites. a – c, plagioclase±biotite association: a) euhedral slightly zonal plagioclase phenocrysts; b) sieve-textured fragment and euhedral zonal plagioclase crystal in perlite; c) crystal clot composed by biotite and plagioclase phenocrysts. K-feldspar builds cores of the smaller crystals and distinct zones in larger ones; d) pyroxene-containing association with strongly zonal plagioclase phenocrysts. Op, opal-CT

Фиг. 3. Изображения в режим на обратноотразени електрони на различни типове плагиоклазови порфири в Шейновецките риолити. a – c: асоциация плагиоклаз±биотит: a) идиоморфни плагиоклазови фенокристали със слабо изразена зоналност; b) фрагменти със ситовиден строеж и автоморфни зонални плагиоклазови порфири в перлит; c) гломеропорфир, изграден от биотит и плагиоклаз. Централните участъци на по-дребните плагиоклазови кристалчета и ясно обособени зони в по-едрите са от калиев фелдшпат; d) пироксен-съдържаща асоциация - плагиоклази със силно изразен зонален строеж. Op – опал-CT

variation in composition are also present in some of the samples (Fig. 3B). Biotite occurs as fine flakes (<0.8 mm) as the range in its composition (Table 2) is shown in Fig. 4. The accessory minerals detected are magnetite, apatite, zircon and titanite. Fragments of plagioclase phenocrysts are also very abundant. They vary from relatively large (0.6 mm) subhedral fragments from coarse sieve-textured crystals to extremely fine splinters.

The groundmass is cryptocrystalline or microfelsitic (built up of feldspar-quartz

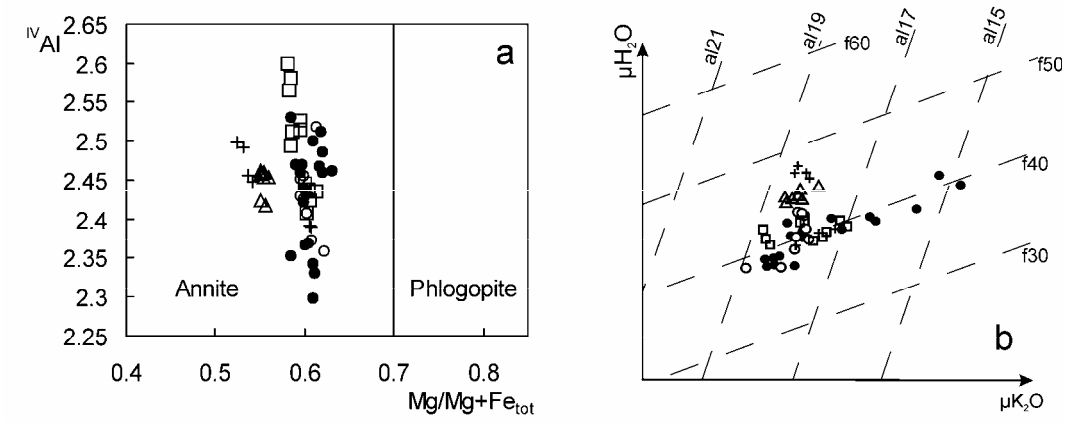

Fig. 4. a) Systematic of biotites from the Sheinovets caldera rhyolites; b) variation of biotite chemistry with regards to the activity of H_2O and K_2O (according to Ivanov, 1974); al=100×Al/(Al+Si+Ti+Mn+Mg+Fe_{tot}), f=100×Fe_{tot}/(Fe_{tot}+Mg). Symbols are the same as in Fig. 2

Фиг. 4. а) Класификация на биотитите в риолитите от Шейновецката калдера; b) Вариации в състава на биотита в координати μH_2O-μK_2O (по Ivanov, 1974); al=100×Al/(Al+Si+Ti+Mn+Mg+Fe_{tot}), f=100×Fe_{tot}/(Fe_{tot}+Mg). Символите са като на фиг. 2

aggregate sometimes enclosing single spherulites), rarely spherulitic. Perlite varieties have glassy groundmass locally rich in plagioclase microliths.

Sanidine+plagioclase+biotite+quartz association

This phenocryst association is found in two bodies only in quantities not preceeding 10-12%. Sanidine (Or_{72-65}) is the main phenocryst occurring as large (2 mm) euhedral to subhedral simply twinned crystals. Plagioclase is also abundant. It forms smaller (1 mm) euhedral or subhedral crystals showing weak normal or reverse zoning and varying in composition between An_{24} and An_{12} (Table 1, Fig. 2B). Biotite is also present and according to the diagrams shown on Fig. 4 it has lower Mg/Mg+Fe_{tot} ratio and seems to have been formed at lower temperature but higher water activity, which is also typical of the altered quartz-bearing rhyolites from the caldera rim. Quartz occurs as fine (<0.5-1 mm) well-rounded crystals showing resorbed and locally deeply embayed margins. Zircon and tiny magnetite are very rare but were also detected.

The ground mass is granophyric, better crystallized compared with quartz-free samples and enriched in anhedral quartz grains.

In these two bodies only, the plagioclase and sanidine phenocrysts were found to be in equilibrium and temperatures of 660 and 675°C (at 1 kbar) were obtained after applying the two-feldspar thermometer of Fuhrman and Lindsley (1988). Temperatures below 700°C are indicated also by the isotherms plotted in Fig. 2. Sanidine present in the other associations is not in equilibrium with associated plagioclases and temperatures could not be calculated.

Plagioclase+biotite+clinopyroxene+sanidine association

Clinopyroxene containing association is detected in a rich in phenocrysts (30%) sample, collected from one of the dykes (Fig. 1).

Plagioclase (less than 1 mm across) is still the most abundant phenocryst often forming crystal clots that can be both free of mafic minerals and biotite, pyroxene and magnetite bearing. Plagioclase forms euhedral to anhedral crystals showing clear zonal texture. Normally two plagioclase phases (An_{69} and An_{41} in a case of biotite+pyroxene+magnetite containing clot and An_{84} and An_{52} - in an only plagioclase containing clot, Fig. 3D, Table 1) build the cores. They are strongly resorbed and mantled by oscillatory-zoned peripheries ranging in composition between An_{66} (or An_{76} if the core is of bitovnite) and An_{32}. The outermost rim is of andesine ($An_{38\text{-}38.5}$). The smaller euhedral plagioclase crystals from the clots do not have resorbed cores but display reverse zoning as obtained An contents vary from An_{51} to An_{33}. Separate plagioclases are also present. They are mainly euhedral to subhedral coarse sieve textured crystals showing no zonal textures and only a weak variation in composition ($An_{39\text{-}31}$). Subhedral fragments sometimes as large as 2 mm of both zonal and sieve-textured plagioclase crystals are extremely abundant. Biotite phenocrysts are also common, as flakes not larger than 1 mm, participating in the crystal clots or dispersed in the groundmass. There is some variation in its composition, as the biotite from the pyroxene containing clots seems to be enriched in ^{IV}Al (Fig. 4, Table 2). Pyroxene ($Wo_{48\text{-}46}En_{40\text{-}37}$, Table 3) occurs as small anhedral grains (less than 1 mm) within the crystal clots or, very rare, singly as large (up to 2.5 mm) euhedral crystals. Separate subhedral sanidine crystals (Or_{69}) were also detected. Magnetite and less apatite are also present. The ground mass is cryptocrystalline.

Discussion

Observed variety in texture and phenocryst associations of Sheinovets caldera lava rocks suggests differences in crystallization history of chemically undistinguishable magma batches successively derived (over a period of about 3 Ma, Fig. 1) from different levels of one reservoir showing gradients in volatile content, temperature, crystal assemblage and degree of contamination by less evolved magma (Ivanova, 2005).

The presence of amphibole phenocrysts in some of the samples indicates magma storage within the amphibole stability field. In the area of Sheinovets caldera that could be the upper water enriched parts of the chamber, located at depth of about 7 km below the surface and pressure of nearly 2 kbar, as calculated using Al content in coexisting plagioclase and amphibole (Ivanova, 2005). Reaching that region the magma had already contained plagioclase and biotite crystals. After some time of amphibole dominated crystallization the magma underwent sufficient decompression that might have resulted in formation of coarse sieve-textured plagioclase crystals (Nielson, Montana, 1992). Final solidification occurred at shallower depths above the amphibole stability field (as indicated by the lack of amphibole microliths in the groundmass) after rapid ascent event prevented amphibole from breaking down. Later these bodies were destructed and large fragments erupted during paroxysmal stages of the explosive activity. Magma batches emplaced within the rim of the caldera also were derived from the upper amphibole-bearing parts of the reservoir but they suffered much slower ascent accompanied by significant cooling and loss of volatiles resulting in decomposition of amphibole and partly of biotite and crystallization of quartz+sanidine.

Solid-state amphibole dehydration occurs in response to the decompression driven escape of water from coexisting melt during very slow ascent or long storage at shallower levels (Rutherford, Hill, 1993). Thus, the existence of another magma holding reservoir at shallow levels or, alternatively, shallowing of the magma reservoir and ascending of its upper parts above the amphibole stability field (not deeper than about 4 km according to the

available data on the amphibole stability, Rutherford, Hill, 1993; Blundy, Cashman, 2001) could be supposed to explain features of the most typically observed in the area plagioclase±biotite containing rhyolites. Ca-rich cores (up to An_{78}) preserved in some of the plagioclase phenocrysts are remnants of incompletely resorbed crystal population originally crystallized in contaminated magma in deeper levels. The small amount of phenocrysts in these bodies it though to suggests near liquidus temperature of erupting magma (Eichelberger et al., 1986) resulting from rapid ascent from relatively small depth. The lack of quartz and sanidine phenocrysts then can be due to both non-eutectic crystallization and longer nucleation-lag times in rhyolitic melts (Naney, Swanson, 1980; Swanson et al., 1989). Additionally, water may also inhibit quartz nucleation by depolymerizing the melt (Marakushev, 1978; Brugger et al., 2003).

Observed zones of almost pure potassium feldspar in plagioclase phenocrysts from some of the samples record periods of significant increase of potassium activity that can result from contamination by high-potassium magma or, more probably, from assimilation of rich in K-containing minerals (K-feldspar, mica) wall rock material.

As it was mentioned above, quartz+sanidine-containing bodies with abundant groundmass quartz can be due to crystallization at very low pressures resulting from slow magma ascent accompanied by significant cooling (Blundy, Cashman, 2001).

Pyroxene-containing crystal association was stable in deeper, probably both hotter and drier parts of the reservoir where significant contamination by more mafic magma must have occurred as recorded in the plagioclase phenocrysts. Observed internal dissolution surfaces associated with compositional amplitudes of over 20% An are thought to reflect significant disturbance of the crystallizing system caused by magma mixing process. The complex zonation patterns detected in larger plagioclase phenocrysts can be explained with crystal transfer between less evolved magma coming from depth (An_{87-84}), host rhyolite (An_{52} and more sodium-rich compositions) and hybrid magma batches (An_{76-66}) that must have existed for some time in the bottom parts of the chamber according to ideas of Tepley et al. (1999). Observed differences in biotite chemistry (Fig. 4) could also be due to the crystallization from chemically distinct magma batches.

Conclusions

Two levels of magma storage and differences in magma ascent rate can explain observed variety in phenocrysts assemblages detected in the Sheinovets caldera rhyolites. Both plagioclase+biotite and sanidine+quartz (±amphibole) containing lava rocks erupted during Priabonian when the near-by Lozen volcano was formed. Possible con-nection between these eruptive events is proposed in Ivanova et al. (2001). In the end of Priabonian the area studied became a field of explosive activity (during which fragments of amphibole-bearing subvolcanic bodies were ejected) resulted in Sheinovets caldera collapse (Ivanova et al., 2000, 2001). Shallow depths of magma crystallization are required caldera subsidence by roof collapse to occur (Lipman, 1997). Plagioclase±biotite containing lava domes of Rupelian age also indicate shallow levels of magma storage and appear to be connected to the collapse event. The emplacement of later dykes is thought to be tectonically induced (Ivanova, 2005) and observed variation in phenocryst assemblages: plagioclase±biotite, sanidine+plagioclase+biotite+quartz, and plagioclase+ biotite+clinopyroxene+sanidine) can be due to the different rate of magma drainage from different levels of the magma reservoir.

Acknowledgments: The author is obliged to Prof. Dr. W. Richter and Prof. Dr. T. Ntaflos of Institute of Petrology, Vienna University, for invitation and assistance with microprobe analyses. Thanks are also due to W. Füzi and C. Nachtnebel for sample preparation. Tz. Iliev (Geological Institute, Bulgarian Academy of Sciences) is acknowledged for microprobe analyses. Helpful comments of Ass. Prof. Y. Yanev are also highly appreciated.

References

Blundy, J., K. Cashman. 2001. Ascent-driven crystallization of dacite magmas at Mount St Helens, 1980-1986. *Contrib. Mineral. Petrol*., **140**, 631-650.

Brugger, C.R., A.D. Johnston, K.V. Cashman. 2003. Phase relations in silicic systems at one-atmosphere pressure. *Contrib. Mineral. Petrol*., **146**, 356-369.

Eichelberger, J.C., C.R. Carrigan, H.R. Westrich, R.H. Price. 1986. Non-explosive silicic volcanism. *Nature*, **323**, 598-602.

Elkins, L.T., T.L. Grove. 1990. Ternary feldspar experiments and thermodynamic models. *Amer. Mineral*., **75**, 544-559.

Fuhrman, I., P. Lindsley. 1988. Ternary feldspar modeling and thermometry. *Amer. Mineral*., **73**, 201-215.

Ivanov, R. 1960. Der magmatismus in der paläogenen Senkung der Ostrodopen I. Teil – Geolgie. *Trav. géol. Bulgarie, Ser. géochim., gîtes. métal*., **1**, 311-387 (in Bulgarian with German abstract).

Ivanov, V.S. 1974. On the influence of temperature and chemical activity of potassium over biotite composition in granitoides. *Izvestia Acad. Nauk SSSR, Ser. Geol*., **7**, 20-30 (in Russian).

Ivanova, R. 2005. Volcanology and petrology of acid volcanic rocks from the Paleogene Sheinovets caldera, Eastern Rhodopes. *Geochem. Mineral. Petrol*., **42**, 23-45.

Ivanova, R., K. Stoykova, Y. Yanev. 2000. Acid pyroclastic rocks from the Sheinovets caldera, Eastern Rhodopes: Lithostratigraphy, characterristics and age. *Geochem. Mineral. Petrol*., **37**, 47-56.

Ivanova, R., Z. Pecskay, Y. Yanev. 2001. K-Ar age of the volcanic rocks from the Sheinovets caldera, Eastern Rhodopes (South Bulgaria). *C. R. Acad. bulg. Sci*., **54**, 59-62.

Leake, B.E. et al. 1997. Nomenclature of amphiboles: Report of the Subcommittee on amphiboles of the IMA, CNMMN. *Amer. Mineral*., **82**, 1019-1037.

Lipman, P.W. 1997. Subsidence of ash-flow calderas: Relation to caldera size and magma-chamber geometry. *Bull. Volcanol*., **59**, 198-218.

Marakushev, A.A. 1978. Some questions on petrogenesis in the light of the theory of fluid-magma interaction. In: *Problems in Petrology of the Earth Crust and Upper Mantle*. Novosibirsk, Nauka, 65-83 (in Russian).

Naney, M.T., S.E. Swanson. 1980. The effect of Fe and Mg on crystallization in granitic systems. *Amer. Mineral*., **65**, 639-653.

Nielson, S.T., A. Montana. 1992. Sieve-textured plagioclase in volcanic rocks produced by rapid decompression. *Amer. Mineral*., **77**, 1242-1249.

Rutherford, M.J., P.M. Hill. 1993. Magma ascent rates from amphibole breakdown: An experimental study applied to the 1980-1986 Mount St. Helens eruption. *J. Geophys. Res*., **98**, 19667-19686.

Swanson, S.E., M.T. Naney, H.R. Westrich, J.C. Eichelberger. 1989. Crystallization history of Obsidian Dome, Inyo Domes, California. *Bull. Volcanol*., **51**, 161-176.

Tepley, III F.J., J.P. Davidson, M.A. Clynne. 1999. Magmatic interactions as recorded in plagioclase phenocrysts of Chaos Crags, Lassen volcanic center, California. *J. Petrol*., **40**, 787-806.

Wen, S., H. Nekvasil. 1994. SOLVALC: An interactive graphics program package for calculating the ternary feldspar solvus and for two-feldspar geothermometry. *Comp. Geosci*., **20**, 1025-1040.

Yanev, Y. 1995. General characteristics of the Late Paleogene collision volcanism in the Rhodopes. In: B. Aleksiev (Ed.). *Sofia Zeolite Meeting'95*. Intern. Symp., Guide Field Trip, 3-19.

Yanev, Y. 1998. Petrology of the Eastern Rhodopes Paleogene acid volcanism, Bulgaria. *Acta Vulcanol*., **10**, 265-277.

Yanev, Y., B. Karadjova, A. Andreev. 1983. Distribution of alkalies and genesis of the acid effusives in part of East Rhodope Paleogene depression. *Geol. Balcanica*, **13**, 15-44 (in Russian with an English abstract).

Accepted March 15, 2006
Приета на 15. 03. 2006 г.